Manipulation of Majoran Modes in a Double Quantum Dot

Jesus D. Cifuentes[1] and Luis G. G. V. Dias da Silva[1]

[1] *Instituto de Física, Universidade de São Paulo, C.P. 66318, 05315–970 São Paulo, SP, Brazil*

(Dated: December 4, 2018)

(To be written)

I. INTRODUCTION

In the last few decades the interest in the so called Majorana fermions has been increasing. The particle proposed by the physicist Ettore Majorana as the real field solution of the Dirac equation describes a fermion which is its own antiparticle, hence it has no charge nor mass. To the date no fundamental particle with these characteristics has been found. However, theoretical research predicts that Majorana Fermions emerge as quasi-particles at the boundary of certain topological superconductors Kitaev [1]. Recently, the new technological innovations allowed the observation of Majorana signatures in different topological materials[2–5] .

Despite the positive experimental results, their is still certain skepticism about the existence of Majorana Fermions. One of the reasons is that some properties of Majorana quasiparticles like the expected non-abelian statistics have not been measure. This property is of especial interest due to its promising applications in topological quantum computing. The braiding protocol based on Majorana's non-abelian statistics is the key to fault-tolerant quantum computation[6,7].

A promising method to detect majorana modes consists in attaching a Quantum Dot (QD) to the edges of a majorana chain in the topological phase and executing transport measurements through the QD[8] . The majorana mode at the end of the chain then leaks inside the QD[9] which produces a zero-bias conductance peak of half a quanta $\frac{e^2}{2h}$ through the dot. This is a majorana signature which produces half of the expected peak by a regular fermion. Recently, experiments including hybrid Majorana-QD systems have been performed[10] . In addition, the similarity of this phenomenon with the Kondo effect, where the zero-bias conductance peak takes $\frac{e^2}{h}$, motivated the study of combined Kondo-Majorana physics in this system[11,12]. This project revealed the existance of a region of parameters where both, Kondo and Majorana physics, coexist.

This idea has turned on new lights into the design of quantum architectures[13,14] , because todays precise experimental control over the parameters of QDs - energy levels, tunneling couplings, etc. - offers the unique possibility of manipulating the Majorana modes inside multidot systems. The simplest case where Majorana manipulation is possible is in a Double Quantum Dot. So far, no complete analysis of this simple case has been done. The goal of this project is to fill this gap by realizing a full quantum transport study of the effects of coupling a Majorana mode with a Double Quantum Dot.

The idea of using hybrid quantum dot-majorana heteroestructures to implemtent quantum gates has aquired wide interest in the last years. One of the insights of these structures is the posibility of manipunaling Majoranas in multidot systems by shifting the QD gate voltages and Hence the approach is suitable for the implementation of braiding procedures . The simplest system where Majorana manipulation is possible is a Double Quantum Dot (DQD) coupled to a majorana chain. So far, no complete analysis of this simple case has been done. The goal of this project is to fill this gap by realizing a full quantum transport study of the effects of coupling a Majorana mode with a Double Quantum Dot. By tuning the QD gate voltages and the majorana couplings we will be able to probe the mobility of the majorana modes through the dots.

We considered both interacting and non-interacting cases. For interacting systems we used a obtained the exact transport description . On non-interacting models we used a NRG approach. We found that in symmetric couplings In the non-interacting case, we confirmed that shifting the QDs gate voltage induces the Majorana to tunnel only to the other dot. In addition, an indirect coupling of the second dot could cause destructive interference with the Majorana signature. In the interactict-ing case, the NRG simulations confirmed these results and showed that other interacting effects - like Kondo and RKKY[15–17] - could coexist with the Majorana signatures. On the other hand, when only one QD is coupled to the leads and the other Dot is attached to the QD, the Kondo effect is annihilated due to the destructive interference generated by extra dot[18]. Our study includes how the Majorana mode interacts with these two effects.

II. MODEL AND METHODS

We consider the setup shown in Figure 1 in which a Majorana Bound State (MBS) at the edge of Topological Superconductor(TS) is coupled to a double quantum dot (DQD), which is attached to a single metallic lead. The Hamiltonian of this system can be partitioned in four terms: the DQD Hamiltonian H_{DQD} , the Lead Hamiltonian H_{Lead} , the DQD-lead interaction $H_{DQD-Lead}$ and the coupling between the DQD and the Majorana mode H_{M-DQDs} and

$$H = H_{DQD} + H_{Lead} + H_{DQD-Lead} + H_{M-DQD} \quad (1)$$

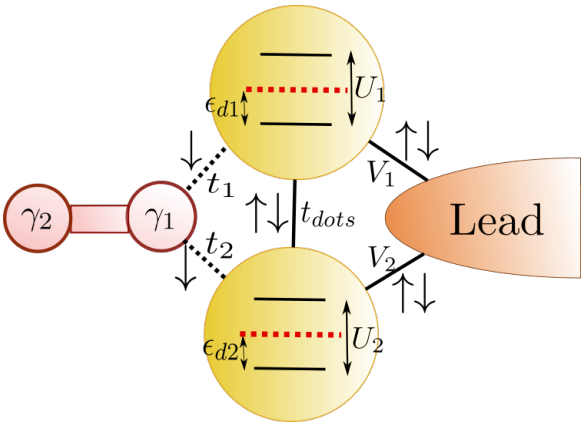

FIG. 1: DQD-Majorana set-up. Solid lines: standard coupling. Dashed lines: majorana spin-↓ effective couplings (6). The atomic energy levels appear inside each QD. Red dashed horizontal lines represent the Fermi level.

The interacting Anderson Model describes the DQD-lead system

$$H_{DQD} = \sum_{i\in\{1,2\}}\sum_{\sigma\in\{\downarrow,\uparrow\}}\left(\epsilon_{di}+\frac{U_i}{2}\right)\hat{n}_{i\sigma}+\frac{U_i}{2}(\sum_{\sigma}\hat{n}_{i\sigma}-1)^2 + \sum_{\sigma\in\{\uparrow,\downarrow\}} t_{dots}(d^\dagger_{1\sigma}d_{2\sigma}+d^\dagger_{2\sigma}d_{1\sigma}), \tag{2}$$

and

$$H_{Lead} = \sum_{\mathbf{k}\sigma}\epsilon_{\mathbf{k}}c^\dagger_{\mathbf{k}\sigma}c_{\mathbf{k}\sigma} \tag{3}$$

$$H_{DQD-Lead} = \sum_{\mathbf{k}\sigma}\sum_{i\in\{1,2\}} V_{i\mathbf{k}}c^\dagger_{\mathbf{k}\sigma}d_{i\sigma}+V^*_{i\mathbf{k}}d^\dagger_{i\sigma}c_{\mathbf{k}\sigma}, \tag{4}$$

where ϵ_{di} is the energy level of Dot i, U_i is the Coulomb repulsion and t_{dots} is the coupling parameter between both QDs. The operator $d^\dagger_{i\sigma}$ creates a particle in Dot i with spin σ and $\hat{n}_{i\sigma} := d^\dagger_{i\sigma}d_{i\sigma}$ is the particle number operator of state i. $c^\dagger_{\mathbf{k}\sigma}$ is the creation operator a particle with momentum $\mathbf{k}$ and spin σ in the lead. $\epsilon_{\mathbf{k}l}$ is the corresponding energy and $V_i(\mathbf{k})$ describes the tunneling coupling between the lead and Dot i .

The majorana modes are modeled as a superposition of the creation and annihilation operators of a spin ↓ particle $f_\downarrow$

$$\gamma_1 := \frac{1}{\sqrt{2}}\left(f^\dagger_\downarrow + f_\downarrow\right), \gamma_2 := \frac{i}{\sqrt{2}}\left(f^\dagger_\downarrow - f_\downarrow\right). \tag{5}$$

This makes possible to define an effective coupling between the Majorana Mode and the DQD by attaching γ_1 with the spin-↓ channel in the QDs

$$H_{M-DQD} = \sum_{i=1}^{2} t_i\left(d^\dagger_{i\downarrow}\gamma_1+\gamma_1 d_{i\downarrow}\right)+\epsilon_M\gamma_1\gamma_2. \tag{6}$$

where t_i is the coupling parameter between the majorana mode and QD i. ϵ_m is the coupling energy between both majorana modes. This effective model is able to reproduce the physical effects of more elaborated couplings[12] such

Ruiz-Tijerina *et al.* showed that this effective coupling is able to reproduce effectively the transport effects of the Kitaev chain in the topological phase is attached to a single QD.

A. Methods

To study the non-interacting case ($U = 0$), we use Zubarev's ballistic transport approach[19] to compute the Green functions associated to both quantum dot operators $(G_{d_1d_1^\dagger}(\omega), G_{d_2d_2^\dagger}(\omega))$. The detailed procedure is included in **??**. The transport equations define a linear system where the Hamiltonian parameters $(t_1, t_2, \epsilon_1 \ldots)$ and the energy ω are taken as fix variables . The flow graph in FIG.2 depicts the linear map associated to the transport in an hybrid Majorana-DQD system (see (**??**)). The energies of each operator are located at the center of the vertexes while the vertex couplings represent the off-diagonal terms. It is possible to observe the Majorana mode divides this graph in two parts, both of them representing a DQD. The upper DQD is conformed by annihilation operators while the lower one is formed by creation operators. The couplings in the lower part are the negative upper parameters. Meanwhile, the majorana fermion is the vertex acting as a connector between both regions.

To simplify the solution of this system we used a graph linear algorithm[20] to speed-up the process of Gauss-Jordan elimination. The idea consists in "popping-out" the vertexes of the graph one-by-one. Each pop-out process most be understood as the Gaussian elimination of the line and the column in the matrix containing that vertex. Depending on the order of elimination of these vertexes different representations of the final polynomial fraction can be obtained. So the real insight of this method is that it allows us to select the order of vertex elimination to obtain the simplest representation of the final this function.

All this process can be observed graphically in figure 2. In the first step we pop-out the extreme vertexes $c_{k,\downarrow}, c^\dagger_{k,\downarrow}, d_{2,\downarrow}, d^\dagger_{2,\downarrow}$ in that order. This condenses the transport information in the vertexes $d_{1,\downarrow}$, $d^\dagger_{1,\downarrow}$ and $f_\downarrow$, such that the energies $\epsilon^{\pm}_{DQD}$ accumulate the information of both double quantum dots while the couplings are modified to $T_\pm$. The last step is to pop-out vertexes

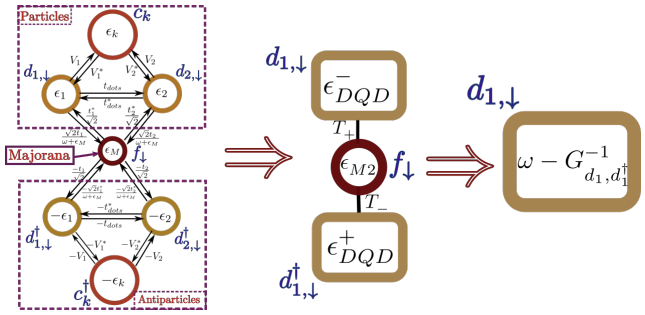

FIG. 2: Transport flow in a DQD majorana system.

$d^\dagger_{1,\downarrow}$ and $f_\downarrow$. At the end of the whole process the energy of the remaining vertex $d_{1,\downarrow}$ contains the green function $G_{d_{1\downarrow}d^\dagger_{1\downarrow}}(\omega)$ giving this very compact expression

$$G_{d_{1\downarrow},d^\dagger_{1\downarrow}}(\omega) = \frac{1}{\omega - \epsilon^+_{DQD} - \frac{\|T_+\|^2}{\omega-\epsilon_{M2}-\frac{\|T_-\|^2}{\epsilon^-_{DQD}}}}. \tag{7}$$

This graph approach turns out to be especially good for Majorana systems since the Majorana fermion is a natural cutting point that divides the graph in two sections, allowing us to exploit the graph structure to simplify the solution of the system. Note also that the spin-↑ green functions can be obtained by replacing the majorana couplings $t_1, t_2 = 0$. The final result will depend on the broadening Γ_i defined by

$$-i\Gamma_i = \sum_{\boldsymbol{k}} \frac{V_i^* V_i}{\omega - \epsilon_{\boldsymbol{k}}}. \tag{8}$$

By convention we will take Γ_1 as the energy unit for the rest of the project. Finally we compute the DOS

$$\rho_{1\sigma}(\omega) = -\frac{1}{\pi}\mathrm{Im}\left[G_{d_{1\sigma},d^\dagger_{1\sigma}}(\omega))\right]. \tag{9}$$

Similar results can be obtain for the DOS of the second $\rho_{2\sigma}$. Comparing these results for both dots at the Fermi energy we will be able to determine which dot exhibits a majorana signature.

B. Non-interacting Case (NRG)

For the non-interacting case we used the Numerical Renormalization Group (NRG) approach[21? ,22]. To improve the efficiency of the code we took advantage of the preserved symmetries, which are spin-↑ particle number $\hat{N}_\uparrow$ and the spin-↓ parity. Spin-↓ particle number is not preserved due to the term $\hat{P}_\downarrow = \pm$ (+ even, − odd). To implement the NRG code it is necessary to define a fix coulomb repulsion cut-off energy $D^?$. To unify the units of the interacting and non-interacting case we pick $U = 8.69\Gamma_1$ and we let $D = 2U_1 = 17.3\Gamma_1$. The final spectral functions are then computed with the Density Matrix Renormalization Group (DM-NRG) approach[23].

III. CONCLUDING REMARKS

Conclusion goes here.

ACKNOWLEDGMENTS

The authors thank Edson Vernek for enlightening discussions. L.G.G.V.D.S. acknowledges financial support by CNPq (grants No. 307107/2013-2 and 449148/2014-9), and FAPESP (grant No. 2016/18495-4).

[1] A. Y. Kitaev, Physics-Uspekhi **44**, 131 (2001).
[2] V. Mourik, K. Zuo, S. M. Frolov, S. R. Plissard, E. P. a. M. Bakkers, and L. P. Kouwenhoven, Science **336**, 1003 (2012).
[3] A. Das, Y. Ronen, Y. Most, Y. Oreg, M. Heiblum, and H. Shtrikman, Nature Physics **8**, 887 (2012).
[4] M. T. Deng, C. L. Yu, G. Y. Huang, M. Larsson, P. Caroff, and H. Q. Xu, Nano Letters **12**, 6414 (2012).
[5] H. Zhang, C.-X. Liu, S. Gazibegovic, D. Xu, J. A. Logan, G. Wang, N. van Loo, J. D. S. Bommer, M. W. A. de Moor, D. Car, R. L. M. Op het Veld, P. J. van Veldhoven, S. Koelling, M. A. Verheijen, M. Pendharkar, D. J. Pennachio, B. Shojaei, J. S. Lee, C. J. Palmstrm, E. P. A. M. Bakkers, S. D. Sarma, and L. P. Kouwenhoven, Nature **556**, 74 (2018).
[6] A. Y. Kitaev, Annals of Physics **303**, 2 (2003), arXiv: quant-ph/9707021.
[7] S. D. Sarma, M. Freedman, and C. Nayak, npj Quantum Information **1**, 15001 (2015).
[8] D. E. Liu and H. U. Baranger, Physical Review B **84** (2011), 10.1103/PhysRevB.84.201308, arXiv: 1107.4338.
[9] E. Vernek, P. H. Penteado, A. C. Seridonio, and J. C. Egues, Physical Review B **89**, 165314 (2014).
[10] M. T. Deng, S. Vaitiekenas, E. B. Hansen, J. Danon, M. Leijnse, K. Flensberg, J. Nygard, P. Krogstrup, and C. M. Marcus, Science **354**, 1557 (2016).
[11] M. Lee, J. S. Lim, and R. Lopez, Physical Review B **87**, 241402 (2013).
[12] D. A. Ruiz-Tijerina, E. Vernek, L. G. G. V. Dias da Silva, and J. C. Egues, Physical Review B **91**, 115435 (2015).
[13] M. Barkeshli and J. D. Sau, arXiv:1509.07135 [cond-mat, physics:quant-ph] (2015), arXiv: 1509.07135.
[14] T. Karzig, C. Knapp, R. M. Lutchyn, P. Bonderson, M. B. Hastings, C. Nayak, J. Alicea, K. Flensberg, S. Plugge,

Y. Oreg, C. M. Marcus, and M. H. Freedman, Physical Review B **95**, 235305 (2017).
[15] M. A. Ruderman and C. Kittel, Physical Review **96**, 99 (1954).
[16] T. Kasuya, Progress of Theoretical Physics **16**, 45 (1956).
[17] K. Yosida, Physical Review **106**, 893 (1957).
[18] L. G. G. V. Dias da Silva, N. Sandler, K. Ingersent, and S. E. Ulloa, Physica E: Low-dimensional Systems and Nanostructures **40**, 1002 (2008).
[19] D. N. Zubarev, Soviet Physics Uspekhi **3**, 320 (1960).
[20] D. A. Spielman, *Algorithms, Graph Theory, and Linear Equations in Laplacian Matrices*, Proceedings of the International Congress of Mathematicians (2010).
[21] K. G. Wilson, Reviews of Modern Physics **47**, 773 (1975).
[22] M. Sindel, *Numerical Renormalization Group studies of Quantum Impurity Models in the Strong Coupling Limit*, Text.PhDThesis, Ludwig-Maximilians-Universitt Mnchen (2005).
[23] W. Hofstetter, Physical Review Letters **85**, 1508 (2000).

Appendix A: Computation of the Green Function

In Zubarev's fermionic ballistic transport approach[19] the green functions associated to two operators $A(t)$, $B(t)$ is defined as that Fourier transform of the time-ordered anti-commutator of A and B

$$G_{A,B}(\omega) = \mathcal{F}\left\{\mathcal{T}\left[\{A(t), B(t')\}\right]\right\}(\omega)\,. \tag{A1}$$

The Fourier transform of Schrodinger evolution determines the transport equations

$$\omega G_{A,B}(\omega) = \delta_{A^\dagger,B} + G_{[A,H],B}(\omega). \tag{A2}$$

We can apply this to Hamiltonian (1) by replacing A and B by the creation and annihilation operators. To simplify the complexity of the system we fix $B = d^\dagger_{1\downarrow}$. In addition note that the transport equations for $f_\downarrow$ and $f^\dagger_\downarrow$ are

$$(\omega - \epsilon_M)\, G_{f_\downarrow, d^\dagger_{1\downarrow}}(\omega) = \frac{t}{\sqrt{2}}\left(G_{d_{1\downarrow}, d^\dagger_{1\downarrow}}(\omega) - G_{d^\dagger_{1\downarrow}, d^\dagger_{1\downarrow}}(\omega)\right) \tag{A3}$$

$$(\omega + \epsilon_M)\, G_{f^\dagger_\downarrow, d^\dagger_{1\downarrow}}(\omega) = \frac{t}{\sqrt{2}}\left(G_{d_{1\downarrow}, d^\dagger_{1\downarrow}}(\omega) - G_{d^\dagger_{1\downarrow}, d^\dagger_{1\downarrow}}(\omega)\right), \tag{A4}$$

which allows us to take $G_{f^\dagger_\downarrow, d^\dagger_{1\downarrow}}(\omega) = \frac{\omega+\epsilon}{\omega-\epsilon} G_{f^\dagger_\downarrow, d^\dagger_{1\downarrow}}(\omega)$. Therefore, we can eliminate $G_{f^\dagger_\downarrow, d^\dagger_{1\downarrow}}(\omega)$ from the equations even before we start Gauss-Jordan process.

Writing the other equations we obtain the linear system

$$T\vec{G}_{d^\dagger_1} = \hat{e_1} \tag{A5}$$

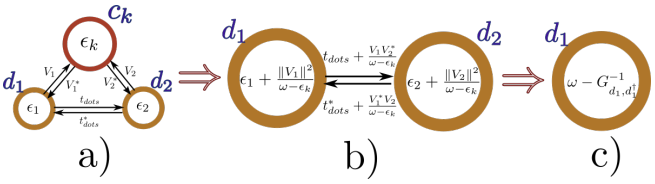

FIG. 3

where T is the transport matrix

$$\begin{bmatrix}
\omega-\epsilon_1 & -V_1^* & -t_{dots} & \frac{-t_1}{\sqrt{2}} & 0 & 0 & 0 \\
-V_1 & \omega-\epsilon_k & -V_2 & 0 & 0 & 0 & 0 \\
-t^*_{dots} & -V_2^* & \omega-\epsilon_2 & \frac{-t_2}{\sqrt{2}} & 0 & 0 & 0 \\
\frac{-\sqrt{2}t_1^*}{\omega+\epsilon_M} & 0 & \frac{-\sqrt{2}t_2^*}{\omega+\epsilon_M} & \omega-\epsilon_M & \frac{\sqrt{2}t_2^*}{\omega+\epsilon_M} & 0 & \frac{\sqrt{2}t_1^*}{\omega+\epsilon_M} \\
0 & 0 & 0 & \frac{t_2}{\sqrt{2}} & \omega+\epsilon_2 & V_2^* & t^*_{dots} \\
0 & 0 & 0 & 0 & V_2 & \omega+\epsilon_k & V_1 \\
0 & 0 & 0 & \frac{t_1}{\sqrt{2}} & t_{dots} & V_1^* & \omega+\epsilon_1
\end{bmatrix}, \tag{A6}$$

$\vec{G}_{d^\dagger_1}$ is the column vector

$$[G_{d_{1\downarrow},d^\dagger_{1\downarrow}}(\omega), G_{c_{k\downarrow},d^\dagger_{1\downarrow}}(\omega), G_{d_{2\downarrow},d^\dagger_{1\downarrow}}(\omega), G_{f_\downarrow,d^\dagger_{1\downarrow}}(\omega), G_{d^\dagger_{2\downarrow},d^\dagger_{1\downarrow}}(\omega), G_{c^\dagger_{k\downarrow},d^\dagger_{1\downarrow}}(\omega), G_{d^\dagger_{1\downarrow},d^\dagger_{1\downarrow}}(\omega)]^T$$

and $\hat{e_1}$ is the vector with entries $\hat{e}_{1_n} = \delta_{1n}$.

The graph associated to this matrix is the one in FIG.2. The energies inside each vertex are given by subtracting the corresponding diagonal term from ω . The couplings are just the negative of the off-diagonal terms.

1. The Double Quantum Dot

To explain the process of Gaussian elimination we will obtain the green function for the case without Majorana fermion ($t_1 = t_2 = 0$). The transport matrix for this system is

$$\begin{bmatrix}
\omega-\epsilon_1 & -V_1 & -t_{dots} \\
-V_1^* & \omega-\epsilon_k & -V_2 \\
-t^*_{dots} & -V_2^* & \omega-\epsilon_2
\end{bmatrix}. \tag{A7}$$

The graph associated to this matrix can be observed in FIG3.a). To eliminate the vertex c_k we just need to subtract from (A7) the rank-1 matrix that cancels the row and the column corresponding to c_k. This matrix is

$$\begin{bmatrix}
\frac{V_1^* V_1}{\omega-\epsilon_k} & -V_1^* & \frac{V_2 V_1^*}{\omega-\epsilon_k} \\
-V_1 & \omega-\epsilon_k & -V_2 \\
\frac{V_2^* V_1}{\omega-\epsilon_k} & -V_2^* & \frac{V_2^* V_2}{\omega-\epsilon_k}
\end{bmatrix}. \tag{A8}$$

The result of (A7) - (A8) is

$$\begin{bmatrix}
\omega-\epsilon_1-\frac{V_1^* V_1}{\omega-\epsilon_k} & 0 & -t_{dots}-\frac{V_2 V_1^*}{\omega-\epsilon_k} \\
0 & 0 & 0 \\
-t^*_{dots}-\frac{V_2^* V_1}{\omega-\epsilon_k} & 0 & \omega-\epsilon_2-\frac{V_2 V_1^*}{\omega-\epsilon_k}
\end{bmatrix} \tag{A9}$$

which is depicted by the graphs in FIG.3.b). The next step is to pop-out the vertex d_2 following the same procedure. At the end, the energy inside the vertex d_1 will be

$$\epsilon_{DQD} = \epsilon_1 + \sum_{\mathbf{k}} \frac{V_1 V_1^*}{\omega - \epsilon_{\mathbf{k}}} + \frac{\left\| t_{dots} + \sum_{\mathbf{k}} \frac{V_1 V_2^*}{\omega - \epsilon_{\mathbf{k}}} \right\|^2}{\omega - \epsilon_2 - \sum_{\mathbf{k}} \frac{V_2 V_2^*}{\omega - \epsilon_{\mathbf{k}}}} \quad \text{(A10)}$$

and the green function of $G_{d_1 d_1^\dagger}(\omega)$ in a DQD will be given by $\frac{1}{\omega - \epsilon_{DQD}}$ (see FIG.3.c)).

2. Solution of the transport equations

The previous procedure can be generalized into the following algorithm:

1. To compute the transport equations with the second term fixed in the creation operator of the dot.
2. To set up the graph associated to the trasport system.
3. To pop out the vertexes of the graph. Each pop-out proces carries the following steps.
   (a) To compute the extra-terms in the energies and couplings based on the walks passing through the vertex that will be popped out.
   (b) To eliminate this vertex from the graph.
   (c) To iterate till there is just one vertex.
4. To invert the last energy to obtain the final green function of the dot.

To solve the general case we start with the graph in FIG.2 and we pop out the vertexes $c_k, c_k^\dagger, d_{2,\downarrow}$ and $d_{2,\downarrow}^\dagger$ in that order. The energies associated to $d_{1,\downarrow}$ and $d_{1,\downarrow}^\dagger$ will be similar to (A10) giving

$$\epsilon_{DQD}^{\pm} = \pm\epsilon_1 + \sum_{\mathbf{k}} \frac{V_1 V_1^*}{\omega - \epsilon_{\mathbf{k}}} + \frac{\left\| \pm t_{dots} + \sum_{\mathbf{k}} \frac{V_1 V_2^*}{\omega - \epsilon_{\mathbf{k}}} \right\|^2}{\omega \pm \epsilon_2 - \sum_{\mathbf{k}} \frac{V_2 V_2^*}{\omega - \epsilon_{\mathbf{k}}}}. \quad \text{(A11)}$$

There is also a correction in the couplings between the majorana mode and $d_{1,\downarrow}$, $d_{1,\downarrow}^\dagger$ given by

$$T_{\pm} = \pm t_1 \pm t_2 \frac{\left(\pm t_{dots} + \sum_{\mathbf{k}} \frac{V_1 V_2^*}{\omega - \epsilon_{\mathbf{k}}} \right)}{\omega \pm \epsilon_2 \pm \sum_{\mathbf{k}} \frac{V_2 V_2^*}{\omega - \epsilon_{\mathbf{k}}}}. \quad \text{(A12)}$$

Finally since the Majorana is in contact with Dot 2, there is an extra-term appearing in the majorana energy given by

$$\epsilon_{M2} = \omega - \epsilon_M - \frac{\frac{\omega}{\omega + \epsilon_M} \|t_2\|^2}{\omega - \epsilon_2 - \sum_{\mathbf{k}} \frac{V_2 V_2^*}{\omega - \epsilon_{\mathbf{k}}}} - \frac{\frac{\omega}{\omega + \epsilon_M} \|t_2\|^2}{\omega + \epsilon_2 - \sum_{\mathbf{k}} \frac{V_2 V_2^*}{\omega + \epsilon_{\mathbf{k}}}}. \quad \text{(A13)}$$

With all the terms of the graph in FIG.2.b) computed, it only remains to pop out vertexes $d_1^\dagger$ and $f_\downarrow$ in that order to obtain the green function in equation (7).